

INTERNATIONAL SOCIETY FOR SOIL MECHANICS AND GEOTECHNICAL ENGINEERING



This paper was downloaded from the Online Library of the International Society for Soil Mechanics and Geotechnical Engineering (ISSMGE). The library is available here:

<https://www.issmge.org/publications/online-library>

This is an open-access database that archives thousands of papers published under the Auspices of the ISSMGE and maintained by the Innovation and Development Committee of ISSMGE.

Mexico City deep eastern drainage tunnel

M.A. Aguilar-Téllez & R. Méndez-Marroquin

Ingenieros Civiles Asociados, Mexico

J.L. Rangel-Núñez

Universidad Autónoma Metropolitana, Mexico

M. Comulada-Simpson & U. Maidl

Maidl Tunnel Consultants, Mexico

G. Auvinet-Guichard

Universidad Nacional Autónoma de México

ABSTRACT: The Eastern Drainage Tunnel project (Túnel Emisor Oriente, TEO) of Mexico City, a deep drainage system for mixed storm water and sewage, with a length of 62 km and interior diameter of 7 m, is being built mainly through lacustrine, alluvial and volcanic soil deposits with a wide range of mechanical characteristics and, along some short stretches, through volcanic rocks. The tunnel's construction also requires excavating 24 shafts with 12–16 m interior diameter and depth ranging from 28 to 155 m. The poor properties of some of the soils encountered, their expected seismic response, the foreseeable effects of regional subsidence on the tunnel in the lacustrine zone, and the high water pressure registered in some geological formations make this project particularly challenging. This paper describes the main features of the project, presents a brief summary of the soil properties, and discusses briefly the geotechnical criteria and analysis methods that were adopted for the design of the typical shafts and tunnel sections, as well as some of the construction methods that are being implemented.

1 INTRODUCTION

The Mexico City valley is a closed basin without a natural water outlet. As a matter of fact, Mexico City was originally built on a small island of the Texcoco lake. Starting in the XVII Century, large artificial dewatering works were undertaken to avoid recurrent flooding of the city (Auvinet, 2010). The Nochistongo trench was opened in 1789 in the northern part of the valley and, in 1900, the Gran canal with a length of 47.5 km leading to the Tequisquiác tunnel was inaugurated. Due to the growth of the urban area and to the pumping-induced general subsidence of the lacustrine zone of the valley, this system soon proved to be inadequate. The Gran canal progressively lost most of its capacity to operate by gravity flow. From 1967 to 1975, a deep drainage tunnel known as Túnel Emisor Central (TEC) with an original capacity of 290 m³/s was built as part of a new deep drainage system (Ref. 03). To reduce the city's vulnerability to flooding in case of problems in the TEC and in order to attend drainage requirements in newly populated areas, it has been considered necessary to build a second deep

drainage tunnel, known as Túnel Emisor Oriente (TEO). This new tunnel will introduce a welcome degree of redundancy in the drainage system, allowing maintenance works to be performed on existing installations. This is the largest civil work being built in Mexico now and probably the largest tunnel in the world built in soft soils.

This paper presents the main features of the project, describes briefly the geological-geotechnical conditions prevailing along the tunnel and discusses the geotechnical criteria and analysis methods adopted for design. Two main aspects are enhanced in this presentation: problems related to construction in the very soft lacustrine clays of Mexico City, affected by regional subsidence and presenting seismic amplification, and the construction of deep parts of the tunnel (down to 150 m) in areas with water pressure as high as 0.75 MPa.

2 GENERAL DESCRIPTION OF THE PROJECT

The TEO is being built in the northeastern part of the Mexico City valley. This tunnel is 62 km

long with interior diameter of 7 m and exterior diameter of 8.4 m for the first 21 km and 8.6 m for the rest of the tunnel. The slope in the north direction is initially 0.19%, reduced to 0.16% after the km 13+460 section (Fig. 1).

Overburden thickness over the tunnel's crown varies from 28 m in the south part (L-0) to 155 m close to the north exit (L-20). Due to the tunnel's length and depth, a wide range of geomaterials are encountered: soft plastic lacustrine clays submitted to regional consolidation and to seismic amplification in the south part, sandy and clayey soils of alluvial or volcanic origin with higher shear strength and lower compressibility in the central part and finally, highly consolidated soils with lenses of boulders inserted in a clayey and silty matrix in the north part. Locally, basaltic lava flows will be encountered. Close to the north end of the tunnel, an aquifer with pressures as high as 0.75 MPa has been detected.

The TEO is being constructed using seven Tunnel Boring Machines (TBM) of the Earth Pressure Balance type (EPBS) and 24 deep shafts will also be constructed, five with internal diameter of 16 m (for assembly and disassembly of TBM) and the rest of 12 m (for operation and maintenance of the tunnel). The distance between contiguous shafts is typically 2.5 km, depth varying from 28 to 155 m. The TEO's north portal is located near the

TEC outlet, and in both cases water is discharged into El Salto River, Hidalgo State.

The construction procedure of the shafts varies depending on the soil profile. Three different construction methods are typically used: 1) walls cast in place for the shaft's entire depth, 2) mixed procedure (wall cast in place down to a certain depth followed by construction with conventional techniques in deeper competent materials (Fig. 2) and 3) use



Figure 1. General layout of the Túnel Emisor Oriente (Google-Earth, 2011).

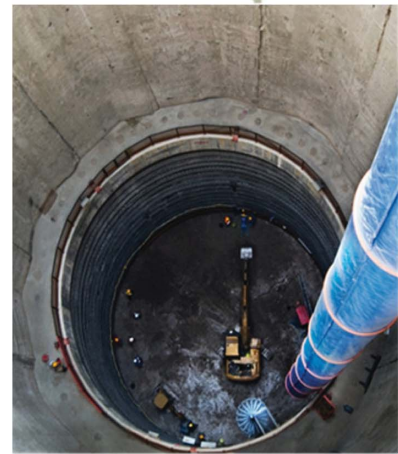
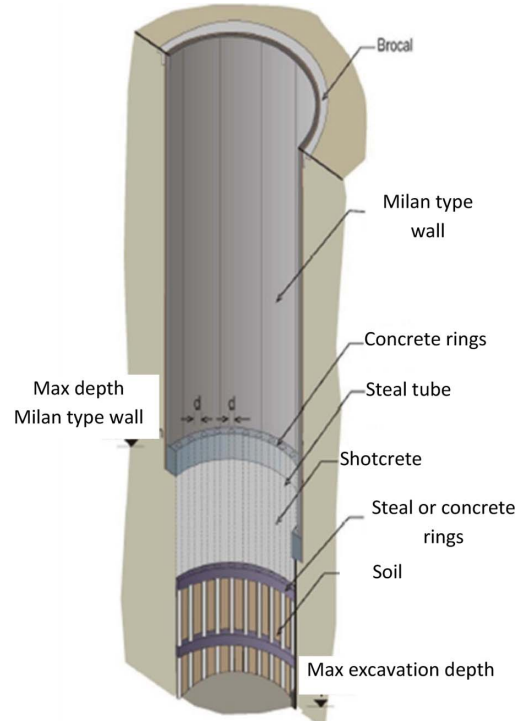


Figure 2. Construction process and lining of shafts (Contreras *et al.*, 2010).

of conventional techniques for the shaft's entire depth.

The tunnel support system (Fig. 3) consists of a primary lining constituted by prefabricated concrete segments and a secondary reinforced concrete lining, cast in place at a second stage. Between shafts L-0 and L-10 (km 21+635.101) the tunnel's exterior diameter is 8.4 m, and the thickness of both the primary and secondary linings is 0.35 m (Fig. 3a); from L-10 to the portal, the exterior diameter is 8.6 m and the thickness of both primary and secondary linings is 0.4 m (Fig. 3b).

For construction purposes, the TEO was divided in six parts (Fig. 1). I: shafts L-0 to L-5, 10.1 km; II: shafts L-5 to L-10, 11.6 km; III: shafts L-10 to L-13, 9.2 km; IV: shafts L-13 to L-17, 10.2 km; V: shafts L-17 to L-20, 8.6 km and VI: shafts L-20 to portal, 12.4 km. These stretches do not correspond to any particular geological or geotechnical zoning.

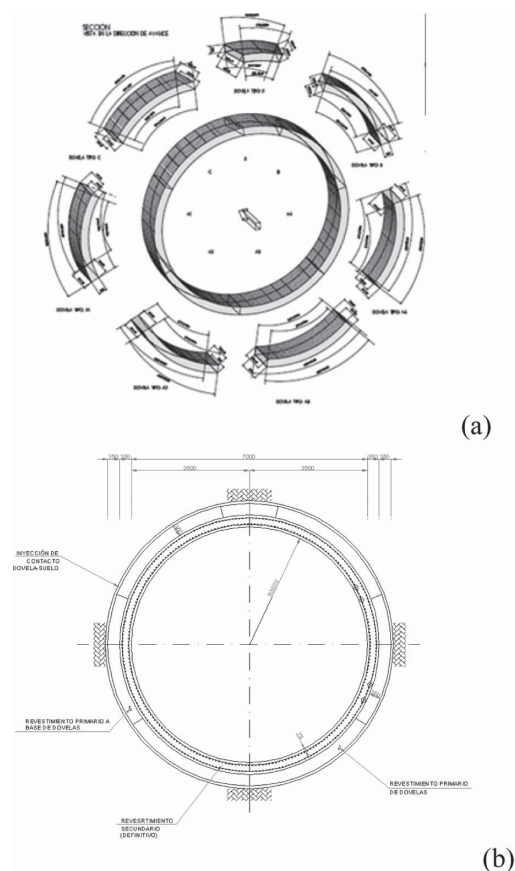


Figure 3. Tunnel support system: primary (a) and combined (b) linings.

3 GEOLOGICAL AND GEOTECHNICAL EXPLORATION

The geological and geotechnical exploration campaign was very ambitious; close to 250 borings (25,000 m) were performed. The campaign was divided into three stages: primary, principal and detailed exploration; some exploration works are still under way.

The following exploration methods have been used:

- Borings: Standard Penetration Test (SPT) and Cone Penetration Test (CPT)
- Soil sampling: Shelby and Denison tubes and triple swivel sampler
- In situ testing: piezometers, permeability tests, pressuremeter, phicometer tests
- Geophysical methods: Cross-hole and SPAC compression and shear wave velocity profile measurements
- Laboratory testing: index and mechanical properties.

Difficulties were encountered for deep explorations (from 100 to 200 m), particularly for undisturbed sampling of silty sand with gravels, clayey silts with sand, and volcanic tuffs. Therefore, in many cases, in situ tests were preferred.

Special studies were also performed to assess the rate of regional subsidence in the lacustrine zone, for the characterization of aquifers and aquitards, for environmental impact, *etc.*

The interpretation of the soil exploration and specialized studies was a challenging task, based mainly on geological maps of the Mexico valley (Mooser *et al.*, 1996). Correlation, estimation and simulation analyses were performed along the tunnel, using geostatistical methods (Auvinet, 2002) in order to assess spatial variability of the geomaterials (Fig. 4) (Juárez *et al.*, 2010).

4 GEOLOGICAL AND HYDRAULIC CONDITIONS

The TEO course was defined trying to minimize hard rock excavation and overburden thickness. As a consequence, the tunnel initially crosses through poorly consolidated Quaternary deposits of the northern part of the Mexico basin along the first 40 km, and then through tertiary tuffs from the consolidated Nochistongo mountain range along 21.3 km.

4.1 General geology

From south to north, in the first 2.5 km the tunnel will be excavated through Quaternary lacustrine

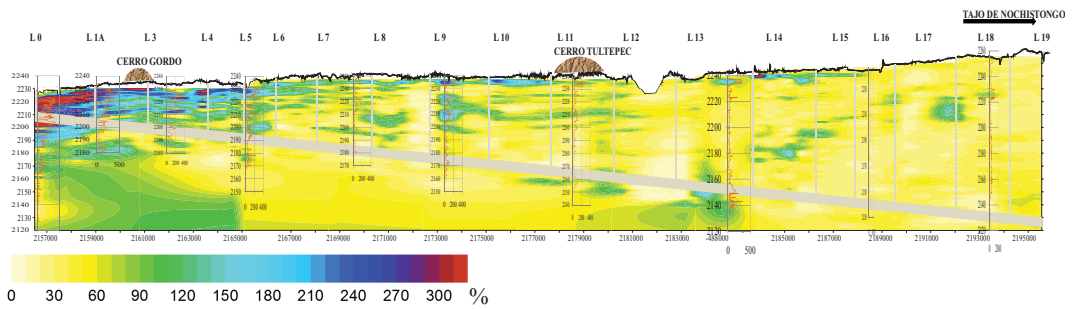


Figure 4. Soil water content in field along the tunnel, as estimated by geostatistical methods.

deposits of the Mexico basin, and then it will cut through a Pliocene formation of the Nochistongo mountain range. Next, the tunnel passes through Pliocene lacustrine deposits of the Taxhimay formation which are divided into tectonic blocks covered by alluvial fans. Some basaltic lava flows will be encountered occasionally (Fig. 5).

4.2 Geological formations

The tunnel will cross six different main formations, namely:

1. Lacustrine Formation of the Mexico basin (upper Quaternary, 300,000 years old; km 0 to 21+140; strata 1, green, 2, yellow, and 10, light blue). It consists of clays interbedded with silts and sands derived mostly from rains of acidic pumices during volcanic eruptions, which were deposited in shallow fresh water lakes in layers 1 to 2 m thick. At the south end of the tunnel, excavation will be performed along a 2.5 km stretch of typical Mexico City lacustrine clays. Lenses and hard layers of clastic materials within the clay deposit may tend to deflect the TBM course.
2. Basalt Formation (Quaternary: km 21+140 to 30+300; strata 3, brown, 7, pink, and 9, red): Basaltic lavas and ash from the north flank of the Nochistongo mountain range and Tultepec hill.
These basalt or ash lenses are found within the lacustrine and alluvial deposits. Due to their high permeability and transmissibility, significant water flow is expected.
3. Sub-lacustrine soils formation (km 30+300 to 38+000; stratum 4, light brown). It consists of alluvial soils, i.e. sandy silts with sand lenses, and occasionally fluvial gravels. There is neither tectonic faulting nor significant water flow.
4. Alluvial fans formation (Plio-Quaternary, Nochistongo mountain range: km 38+000 to 40+350; stratum 6, blue). These deposits are

composed of very compact sand and gravel layers. There is no tectonic faulting and permeability and transmissibility are low.

5. Huehuetoca volcanic formation (upper Pliocene: km 40+350 to 46+000; stratum 7, pink). These deposits are contained in alluvial fans from the south flank of the Nochistongo mountain range, and consist of a thick sequence of semi-hard ignimbrite and compact tuffs. Lavas, pyroclastic flows and gravels with boulders could be encountered. There is not evidence of tectonic faults. It is important to note that, at the bottom of this formation, contiguous to the Taxhimay formation, layers of sandy gravels and silty boulders have been detected, where hydraulic loads are important.
6. Taxhimay Formation (middle Pliocene, 2 million years old: km 46+000 to portal; upper 5s, light green; lower 5i, dark green). This is a much consolidated old lacustrine deposit with clay, silty clay, sandy silt, and occasionally layers of pumice or fluvial sands and tuffs. This formation is divided into two units: the lower one is highly consolidated dark green lacustrine clay, the upper one is less consolidated clay. Permeability and transmissibility are low. However, intense tectonic activity has affected the Taxhimay formation, giving rise to the formation of a block structure which increases permeability. Significant amounts of water, suddenly changing from low to high, can be expected.

4.3 Geohydrology

The TEO will intercept three different aquifers:

- Mexico City aquifer. The tunnel will remain in the upper aquitard that confines the deep Mexico City aquifer. This aquitard consists mostly of impervious lacustrine materials such as clays, with lenses or thin layers of silts and sands.

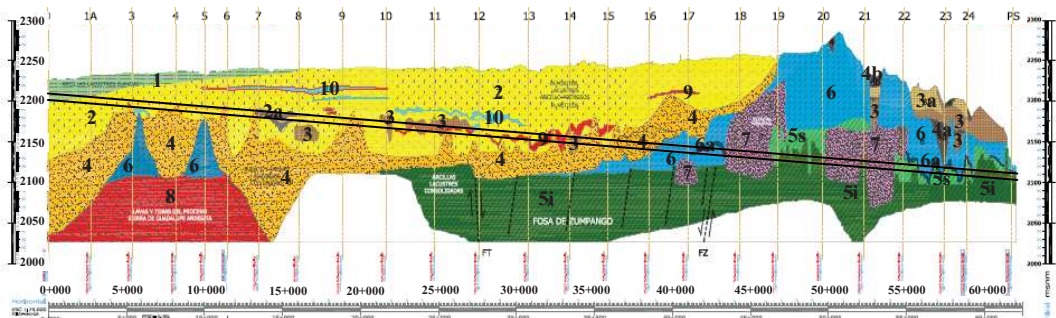


Figure 5. Geology (Mooser, 2010).

- Cuautitlán-Pachuca aquifer, located in Mexico State. This aquifer contains both lacustrine and alluvial sediments as well as rock of volcanic origin.
- Valle del Mezquital aquifer, located in Hidalgo State. This aquifer will be intercepted in the TEO's final stretch.

In both the Mexico City and Cuautitlán-Pachuca aquifers, significant drawdown is observed due to intense water-pumping for local consumption of potable water. Drawdown of the static level registered in some wells can reach 1.3 to 1.6 m/year in the TEO's south part. This has induced, among other effects, subterranean water drainage in the southeast flank of the Sierra de Guadalupe range and the generation of large drawdown cones. On the other hand, in the north part, close to Huehuetoca, in the Mezquital aquifer, drawdown observed is generally less than 0.35 m/year to 1.0 m/year.

The stretch between shafts L-10 and L-18 corresponds to a semi-confined (multilayered) aquifer in lacustrine-type sediments such as sands, silts and clays. At a depth of less than 60 m are perched aquifers that required special attention during the construction of shafts. The hydrostatic level corresponding to the regional aquifer level is found below 65 m. The subsoil is a highly heterogeneous stratified medium with low hydraulic conductivity (1×10^{-4} cm/s). The hydraulic head over the tunnel's crown varies from 5 m to 45 m and estimated potential flow towards the tunnel varies from 0.03 l/s/m to 1.6 l/s/m.

The aquifer between shaft L-18 and exit is semi-confined and located within granular materials such as sands and gravel and sediments of volcanic origin. The granular materials present a medium hydraulic conductivity and are interbedded with fine material with permeability as low as 1×10^{-3} to 1×10^{-4} cm/s, with lateral continuity. The hydraulic head in this stretch was the highest registered along the entire tunnel reaching values as high as

35 m to 75 m over the tunnel keystone, with estimated subterranean flow toward the tunnel of 0.31 to 0.98 l/s/m.

5 GEOTECHNICAL CHARACTERIZATION

From a geotechnical point of view, 95% of the tunnel will be excavated through soils of alluvial-fluvial and volcanic origin and the rest through igneous extrusive rocks such as basalts.

In the first stretch, between shafts L-0 and L1A, the tunnel is located in very compressible clays with low shear strength affected by a pumping-induced consolidation process, known for their amplification of seismic waves. Subsequently, the clayey layers disappear progressively and the tunnel enters a zone of volcanic tuffs formed by sandy silts, or silty sands, occasionally with partially saturated clay, in which the piezometric level has suffered partial or total drawdown, with lenses of sand containing some gravel and very compact volcanic ashes. Between shafts L-10 and L-14 the soil profile changes abruptly and in the tunnel's excavation front it is mixed, with, in the upper part, a basalt flow from Tultepec hill resting on a cemented volcanic ash lying in turn on the volcanic tuff previously mentioned. In this area, piezometric levels are higher. From shaft L-14 to L-16 the tunnel crosses alluvial pre-lacustrine soils composed principally of sandy silts with sand lenses and, locally, fluvial gravel. A specific feature of this zone is that in the lower part of the tunnel section a deformable layer with low shear strength is found, and piezometric levels present an almost total drawdown. Between shafts L-16 and L-19 the soil is a material of alluvial origin, generally sands or silty gravel interbedded with sandy silts, in which, locally, thin layers of boulders contained in a weakly cemented silty matrix are found, with significant water head. From this section onward piezometric pressures increase. From L-19 to the portal the tunnel is

located in the Taxhimay formation, constituted by highly consolidated clays with low deformability and high shear strength; however, the last part of the tunnel is near the contact between the Taxhimay formation and volcanic fans in which a layer of gravel and boulders is found with pore pressures as high as 0.75 MPa and where serious problems for tunnel excavation, control of water and stability of the support system are expected.

In order to give a general idea of the soil quality from the tunneling point of view, Figure 6 presents the depth variation to the tunnel's axis along the tunnel, geostatic total vertical stress and pore pressure, average shear strength, the stability ratio and the safety factor of the tunnel's excavation (Tamez, 1997 and Rangel *et al.*, 2005 and 2007).

The lowest safety factors are obtained in the first stretch of the TEO, which crosses the very soft Mexico City clays presenting high deformability and low shear strength. In this zone, it is necessary to use TBM with pressure control in the excavation front, place primary lining timely, and apply grouting pressure equal to the in situ stress in order to avoid unacceptable settlements of soil surface. Although geo material properties improve as tunnel depth increases, in some zones the tunnel will cross lenses of soft clays with abated pore pressure leading to low safety factors. In these zones, using TBM with the characteristics already described is also necessary. From shaft L-10 onward, but principally between shafts L-19 and L-24, where a layer

of boulders contained in a silt matrix is encountered, hydraulic head with values as high as 0.5 to 0.75 MPa will represent a difficult challenge for the EPBS machines.

A detailed geotechnical description for each tunnel is as follows:

Section I (L-0 to L-5). The overburden thickness varies from 16 to 40 m, and the tunnel is situated mainly in the Mexico City lacustrine zone, where high plasticity clays are found. These highly deformable materials are suffering a consolidation process due to deep water pumping and are known to present strong soil movement amplifications during earthquakes. The water table is found at a depth between 2 and 5 m, and the hydrostatic pressure presents some drawdown in the first 4 km (L-0 to L-3); then the tunnel crosses deeper hard silt and sandy silt deposits with lenses of soft silts with large water pressure drawdown (L-3 to L-5). The main problems from a design point of view are:

- Shaft and tunnel construction in very soft saturated soils, with high deformability and low shear strength.
- Subsidence rate of soil surface around 18 cm/year.
- Seismic amplification
- Presence of cracks in the clay layers.

A typical subsoil profile of this zone is shown in Figure 7, where high water content is correlated to very low undrained shear-resistant and stress-strain modules.

In very soft soils, pressures on the primary lining must be of the same order as those prevailing in geostatic conditions. If this objective is not attained, plastic zones and large radial deformations are generated around the tunnel, leading to unacceptable surface settlement. Furthermore, the primary lining's structural capacity is strongly affected by large radial displacements and by contrasts between horizontal and vertical pressures.

In the first part of this section, the water table is only between 2 and 5 m deep, and no drawdown is registered at depth, so the lining works mainly in compression. However, in the second part of this stretch, water pressures are depleted (Fig. 6) and low ratios (0.7) have developed between the horizontal and vertical stresses, inducing important bending moments in the dowel ring.

The effect of regional subsidence on the primary lining is unfavorable since anisotropic vertical and horizontal effective stresses are induced. For design purposes it was assumed that water pressure drawdown at the hard layer level would increase 9 kN/m² during the 18 month period before the final lining was installed.

Another particular design issue in this zone is the seismic amplification of clay deposits. Figure 8 shows

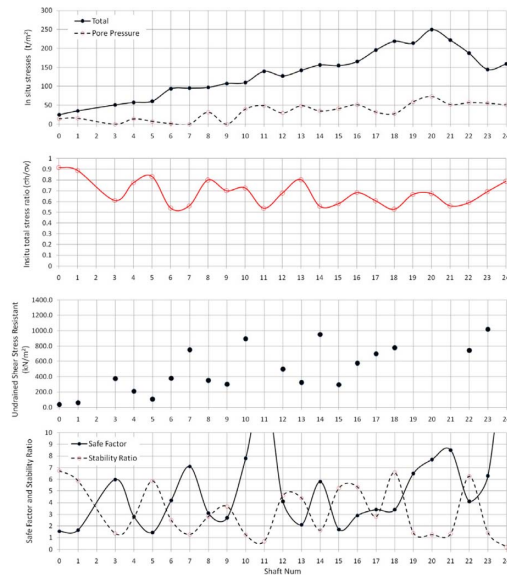


Figure 6. In situ stresses, in situ total stress ratio, undrained shear strength, safety factor according to Tamez (1997) and stability ratio (Rangel, 2005 and 2007).

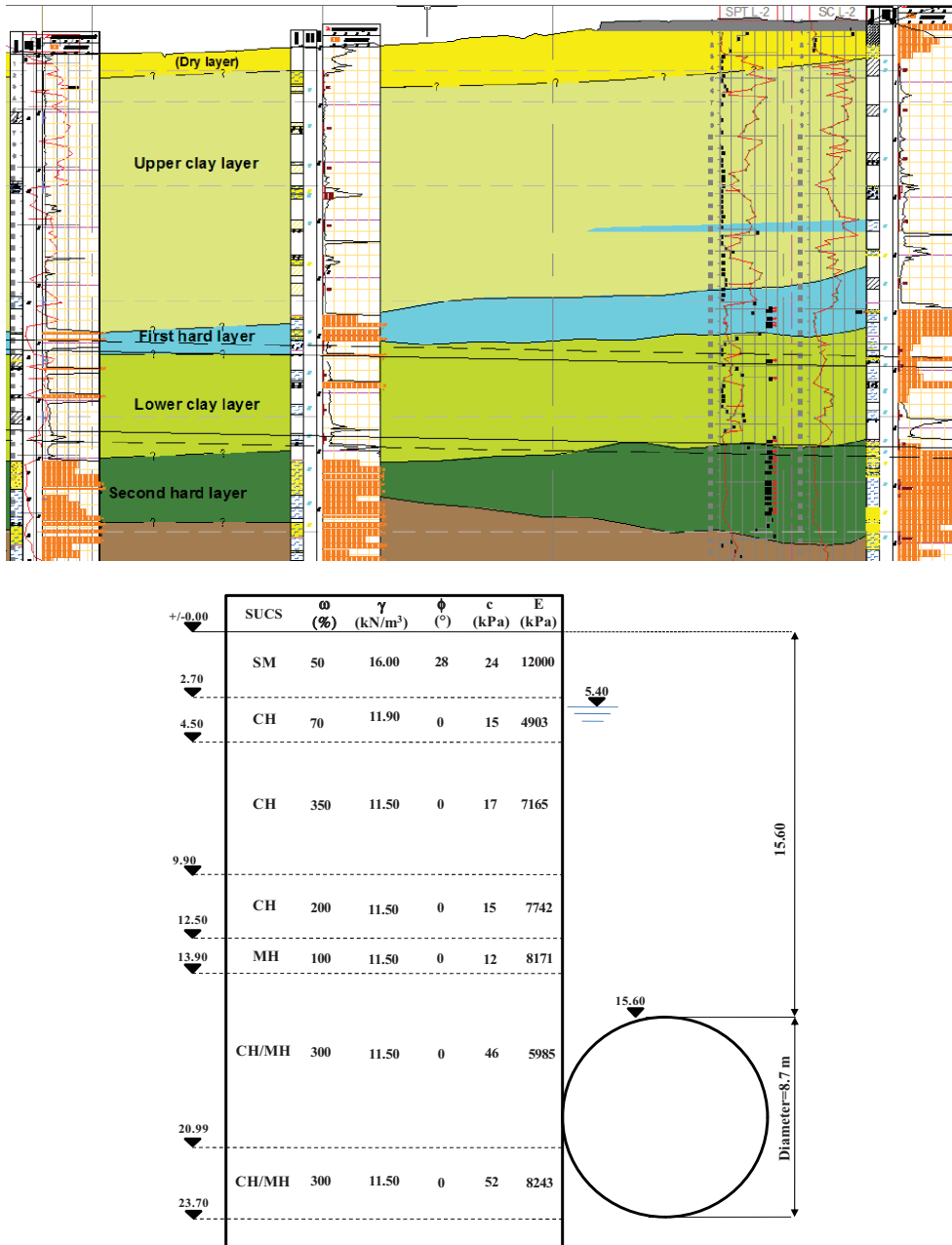


Figure 7. Borings close to shaft L1 (typical soft soil profile).

characteristics of the earthquake and soil deposit design response for Mexico City clay deposits in this TEO zone: a) is the acceleration spectral of the bed rock motion for the Mexico City valley for two return period events (for 47.5 and 475 years, short and long term seismic design periods); b) is the transfer

function for the clay deposit and c) the acceleration spectral at the top of the clay deposit at the beginning of the TEO (L-1). Note a very high amplification, up to 10 times, and free field acceleration at the top of clay deposits around 300 cm/s², which is a typical average value for Mexico City clay deposits.

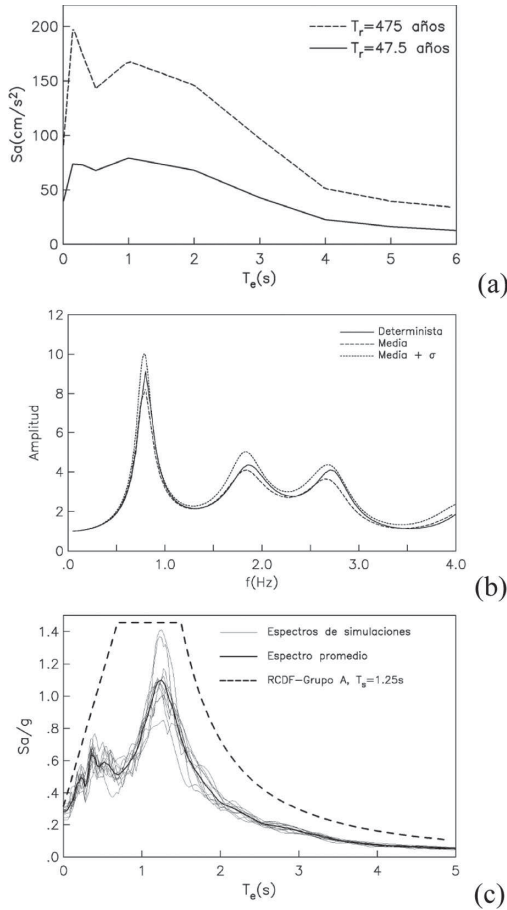


Figure 8. (a) Spectrals of uniform danger in rock for the Mexico valley, (b) transfer function in clayey deposits of the Mexico valley and (c) response spectral in clayey deposits in a return period of 475 years.

Seismic movements affect mainly shafts in the longitudinal direction, and tunnels in the transverse section, but the main effect of earthquakes is in the connection between tunnels and shafts.

Section II (L-5 to L-10). The soil above this part of the tunnel is between 40 m and 70 m thick and consists of volcanic tuffs with low hydraulic conductivity formed by interbedded silts and sandy silts with silty sand lenses. A soft clay lens is found at the tunnel level. Pore pressure in these materials is almost completely depleted, especially between shafts L-6 and L-9 and the ratio between horizontal and vertical stresses is estimated to be as low as 0.7. (Fig. 6). These geostatic stresses and the presence of the soft clay lens are very unfavorable conditions for the primary support's structural work as, given such contrast, the tunnel lining tends to

bend like an oval in the horizontal direction and since the clayey stratum is very deformable, important deformations are also generated on the lining that is formed by dowels. Also, given the important contrast between the deformability of silty strata and that of the clayey lens, high shear stresses are generated at this border on the primary lining. On this stretch there is no soil deposit seismic amplification and the subsidence phenomenon is low.

Section III (L-10 to L-13). Section III, with overburden between 70 and 83 m, is similar to section II since volcanic tuffs are the predominant materials but the hydraulic head tends to increase. This is particularly conspicuous in a basalt lens resting on a sand layer that is found within the silty material. In this zone, a mixed excavation front (saturated basalt and volcanic tuffs) will be encountered. The strong contrast between the moduli of these two materials leads to serious problems in the analysis of lining behavior. Due to depth, geostatic stresses are high. To reduce stresses on the lining, some radial deformation of the soil can be allowed before installation of the support system. This is achieved controlling the pressure in the excavation front and the grouting pressure for the mortar placed in the space between soil and primary lining. However, radial displacements should not lead to development of plastic zones in the soil. Finally, the subsidence and dynamic amplification phenomena are not present in section III. Again, no significant seismic amplification nor noticeable general subsidence are expected.

Section IV (L-13 to L-17). Overburden varies between 83 m and 115 m. The hydraulic head reaches 0.5 MPa and the ratio between total vertical and horizontal stresses is expected to be less than 0.7. The tunnel will cross different geological formations: first clayey and sandy lacustrine deposits with a volcanic ash lens close to the tunnel's crown (shaft L-13); then fine soils and sand with gravel will be found (shafts L-14 and L-15), and at the end of the stretch, the presence of an alluvial fan will probably induce a significant flow of water towards the tunnel (shafts L-16 and L-17). Constructive problems should be expected due to large hydraulic head and sandy layers. On the other hand, due to the low ratio between vertical and horizontal stress, the primary lining will be subjected to important mechanical actions. As far as shafts are concerned, in L-13 alternating sandy silts and silty sands will be found at depths between 70 m and 80 m, and safety factors regarding bottom failure and excavation conditions without support are also expected to be large since the tunnel reaches its largest depth in this area (155 m). To avoid crossing large boulders and fractured volcanic rocks, some significant changes have been introduced in the project based on a large number

of borings. The strategy consists of trying to stay within the Taxhimay formation and sound volcanic rocks as long as possible. In shaft L-20, interbedded silty sand and sandy silts between 62 m and 85 m and clays between 85 m and 112 m may lead to low safety factors during construction. Just as in section III, the tunnel's attack is expected to be of mixed front, especially at the end of the stretch. The consolidation process and seismic amplification here are expected to be low due to the absence of compressible clayey soil deposits. In shaft L-17, clays will be found between 50 m and 60 m and sandy clays will appear between 85 m and 95 m, which will also lead to low safety factors.

Section V (L-17 to L-20). Overburden varies between 115 m and 155 m; the tunnel will cross alluvial fans and the Taxhimay formation, constituted by impervious clayey and sandy deposits with low water content. In this zone there are no highly compressible soils so no consolidation or seismic amplification problems are to be expected.

Section VI (L-20 to L-24). Overburden varies between 80 m and 155 m. The tunnel will be built in the Nochistongo zone of the Tepozotlan range, within the upper and lower Taxhimay formations, alluvial fans and "volcanitas humaredas". A faulting system orthogonal to the tunnel will be encountered, especially in the Taxhimay formation (Fig. 5). Hydraulic head as high as 7.5 MPa has been registered. Geostatic pressures are also expected to be large since the tunnel reaches its largest depth in this area (155 m). To avoid crossing large boulders and fractured volcanic rocks, some significant changes have been introduced in the project based on a large number of borings. The strategy consists of trying to stay within the Taxhimay formation and sound volcanic rocks as long as possible. In shaft L-20, interbedded silty sand and sandy silts between 62 and 85 m and clays between 85 and 112 m may lead to low safety factors during construction. As section III, a mixed excavation front will be encountered, mainly at the end of this section. The consolidation process and seismic amplification here are expected to be low due to the absence of compressible clayey soil deposits.

6 ANALYSIS OF THE TUNNEL SUPPORT SYSTEM

The tunnel support system is built in two stages: a primary lining consisting of six to seven prefabricated segments is being installed in the back part of the tunneling machine as the excavation proceeds while, in a second stage, a final concrete lining is cast using a sliding formwork (Fig. 3).

To represent adequately this constructive process and its mechanical effects in the surrounding

soil and in the lining, evolutionary Finite Element models are used. A structural analysis of the lining is based on the stiffness method. The main stages of the analysis are as follows (Fig. 8):

- i. *Evaluation of geostatic stresses.*
- ii. *Construction of primary lining.* Evaluation of changes in the original stress and strain conditions in the subsoil, including induced pore pressures, and resulting mechanical actions in the tunnel primary lining. Evaluation of changes in these conditions, including dissipation of pore pressures, and of the support system's behavior during the expected life of the primary lining before the final lining is cast (18 months)
- iii. *Construction of secondary lining.* Evaluation of changes in the original stress and strain conditions in the subsoil, and resulting mechanical actions in the tunnel's primary and secondary linings considering an operation period of 50 years, taking into account the probable evolution of the hydraulic conditions within the soil during this period.

6.1 Determination of the geostatic stresses

Initial subsoil stresses (effective, pore pressure and total) are determined based on the soil's volumetric weight, measurements of field pore pressures with open and electronic piezometers for the most unfavorable condition, and evaluating the at rest quotient value by means of the following expressions:

$$k_0 = \begin{cases} \frac{\nu'}{1 - \nu'} & \text{Continuum theory} \\ (1 - \sin \phi') OCR & \text{Jacky (1944) and Meyerhof (1976)} \end{cases}$$

where ν' is the effective Poisson ratio and ϕ' the effective internal friction angle.

In the lacustrine clayey strata the Poisson ratio value was $\nu' \approx 0.5$, whereas in sandy strata (tuffs), agglomerates and rocks it was considered that $0.3 < \nu' < 0.4$.

6.2 Construction of the primary lining

Starting with the subsoil's geostatic conditions and applying surface overburden, changes in the state of stresses and subsoil deformations during the tunnel's excavation with earth pressure balance tunnel boring machines and construction of the primary lining formed by voussoir rings were determined with the two-dimensional Finite Element Method (2D FEM).

At this stage the important points to consider in the construction process modeling are: front pressure, injection pressure, characteristics of mortar or bi-component that is placed in the existing space between lining and medium just after the shield's passing, and the primary lining's rigidity and resistance. For 2D finite element models the soil's radial displacement around the tunnel prior to installing the primary lining is calculated considering the factors previously mentioned, except the last one. A preliminary evaluation of this radial deformation is analyzed by the characteristics curves method, in order to assess the limit conditions of the plastic radii and their corresponding deformations. It is important to mention that this method is widely used in Mexico because of the results obtained in the practice of tunnel-making.

In plastic and very deformable soils located at the start of the outline, it was sought to have the construction process cause very slight changes in the state of geostatic stresses in the surrounding medium in order to diminish to the utmost the surface settlements generated by tunneling; therefore, radial displacements generated on the tunnel's periphery were almost exclusively generated by the deformability of the primary lining's rings, which were less than 1% of the tunnel's diameter, to avoid cracks on the primary support.

For sections where the tunnel has such depth that surface settlements are minimal, a moderate decrease of geostatic stresses is considered, taking care that the plastic zones generated do not indicate failure mechanisms and that radial displacements produced on the lining were always below 1% of tunnel diameter. In these sections, there were problems during the design of the primary lining when the tunnel is located in very deformable soil strata and with null or almost no pore pressure, given that under these conditions the lining's structural work is high for k_0 values indicated before, and loss of the lining's confinement caused by the water. There were also design problems with the mixed excavation front condition, where the contrast between deformation modules of basalt and tuffs is high.

A third case of difficult primary lining design is in the condition of very deep tunnel, with variable coverage between 50 m and 160 m, pore pressure up to 7.5 bars, and located in deformable soils. In this case the construction process and primary support were designed considering an important relaxation of geostatic stresses, and the generation of corresponding plasticization zones around the tunnel. Defining this decrease was critical and it depended on the magnitude of plasticization generated, and the soil's total displacement value on the tunnel's periphery.

Modeling with 2D FEM has the following main analysis stages (Fig. 9):

1. Determination of the state of geostatic stresses and application of surface overburden (0.15 kN/m^2).
- 2 & 3. Evaluation of the change in the state of geostatic stresses due to the shield's passing. At this stage the soil elements are removed from the tunnel's zone and the shield is placed. First, the medium is excavated with a frontal shield weighing 323 kN/m^3 and then the radial displacement induced by the shield's skirting zone, where weight changes to 240 kN/m^3 , is determined. Tunnel emersion and a pore pressure increase are generated at this stage. It is important to point out that the analysis considers pore pressure dissipation as immediate.
4. The primary lining is placed modeled with a continuous cylinder with real dimensions, meaning that the presence of longitudinal or transverse joints is not considered at all, so effective radial and tangential stresses are determined at this stage, pore pressure at the lining-soil interface for different flexibility ratios of the primary lining, EI , and a constant value of axial rigidity, $EA = 8.4 \text{ kN/m}^3$. The detailed structural analysis of the primary lining is done afterward using a model of rigidities formed by two rings, starting with the state of stresses around the tunnel determined at this stage (Comulada and Maidl, 2010). Also, a radial displacement is applied to the soil located in the tunnel's periphery, whose value depends on the characteristics of the filling at the space left by the shield's progress, the injection pressure and the pressure value at the excavation's front, taking care to avoid radial displacements and plastic zones of such magnitude that there are soil failure mechanisms.

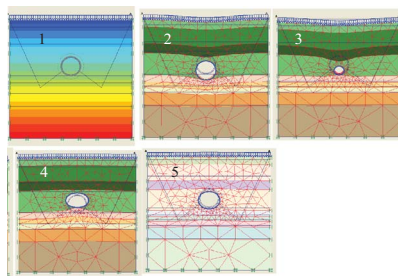


Figure 9. 2D Finite Element Method model for tunneling and placement of primary lining.

5. Primary lining work at 18 months. During this design stage pore pressures are made to descend according to the history of the place. Effective stresses are also determined at the interface located between lining and soil, and pore pressures for later analysis.

Having determined the stresses with incidence on the primary lining at stages 4 and 5 mentioned before (placing the lining and consolidation at 18 months), we proceeded to analyze their behavior taking into account the presence of the longitudinal and transverse sections on the dowel rings. For that, the double ring model developed by Maidl is used (Comulada and Maidl, 2010), in which dowels are modeled with beam elements and the transverse joints with Winkler rotational elements (Fig. 10). The presence of contiguous rings is represented in the model with a second ring connected to the first by Winkler elements. The characteristics of the Winkler elements are determined experimentally. Both rings of the model are supported on Winkler elements so the system is stable, but the rigidity of these elements is insignificant because the state of stresses that have incidence on the support and obtained with the FEM is in equilibrium, so the presence of Winkler elements is only to counteract any maladjustment of numerical origin, and thus the value of the rigidities of these models is very low.

It is important to point out that at the tunnel's first section, limiting radial displacements to low values before placing the support is sought in order to avoid important surface settlement; therefore, the stresses that had incidence on the lining were high and slightly lower than the geostatic ones. For the TEO's final sections, the design strategy was the opposite. In effect, inducing radial displacement on the land before placing the primary support was sought, as well as abating pore pressures in order to diminish pressures acting on that support, but avoiding the generation of important radial displacements and plastic zones around the tunnel.

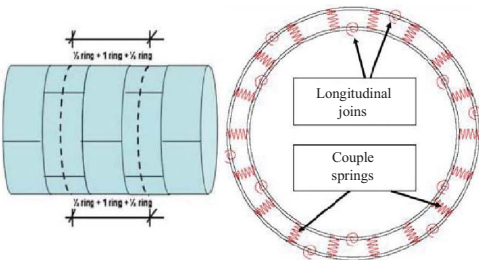


Figure 10. Double ring structural model (Comulada and Maidl, 2010).

Figure 11 shows the results obtained with respect to the primary lining at the end of the analysis. We have the following comments:

- Cases representative of critical conditions obtained for each section are shown with solid blocks. A critical condition is understood as that which presents an inadmissible deformation.
- Variable contractions (1% to 2%) were applied to represent the land's displacement before placing the lining. There are special cases with low values of 0.2% to 0.5% and high values of 3.5% to 4%.
- Flexing rigidity of the continuous support was reduced to values of 10% to 20% to take into account transverse and longitudinal joints between dowels. There are cases, such as in shafts 18 and 20, where the percentage was 40%.
- Axial force on the primary lining was increased from 900 to 6,500 kN/m, as the tunnel's cover was increased, keeping the shear value almost constant at interval 50, and 200 kN/m. The value of the flexing moment did not show a tendency like that of the axial force or the shear; it varied between 30 and 360 kN-m/m.

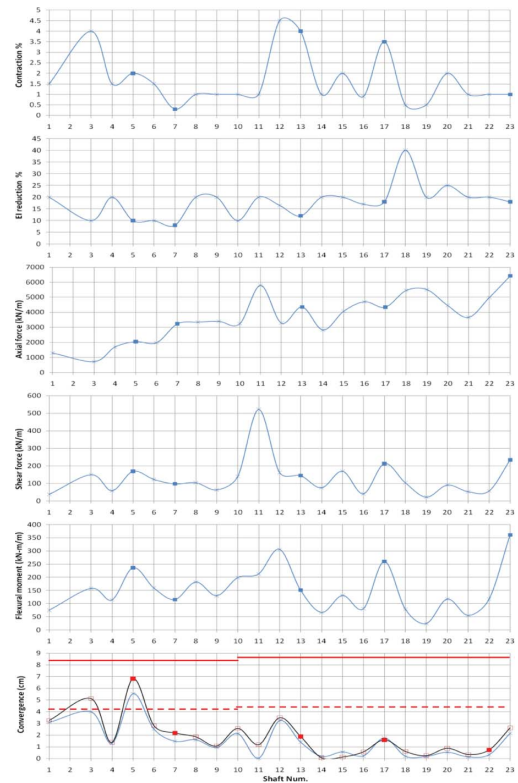


Figure 11. Results obtained from the analysis of TEO temporal lining.

- Horizontal and vertical convergences oscillated but in general were below 0.5% of the tunnel's diameter (4.2 cm and 4.3 cm) except in the cases of shafts L-3 and L-5, whose value was slightly higher although still below 1% of the diameter. This last indicates when the lining begins to crack significantly.

For the analysis of the lining under long term conditions at 18 months (stage 5, Fig. 9), which is the life span assigned to the primary lining, a variable pore pressure abatement between 5 kN/m² and 10 kN/m² was considered, only for the tunnel's initial section (L-0 to L-1A). Also considered is a model with uniform axial load, obtained from the previous state of stresses, with the horizontal pressure decreasing with the abatement proposed at 18 months and using the soil's long term deformability models. This is derived from the field observation indicating that with the tunnel's short term deformation, stress around the tunnel is redistributed uniformly.

6.3 Construction of the secondary lining

The secondary lining is born in a state of stresses caused only by its own weight, although at the soil-primary lining border there is a pseudo-homogenous stress, and the secondary lining will only support stress changes generated in the long term, 50 years, such as remaining stresses caused by placing the secondary lining prior to the primary lining's total stabilization, those caused by the subsidence phenomenon and/or changes in water table levels, and the incidence of seismic waves.

The numerical analysis considers that the primary lining contributes to the tunnel support's work in the long term. For the tuffs and sandy silts zones, apart from the primary lining's remaining work originated by placing the secondary lining at 18 months, two possible long term work conditions are analyzed: total recovery of pore pressures and elimination of that pressure. In the case of lacustrine clays, consolidation development is considered at 50 years. Finally, also considered in all the cases analyzed is the increase of stresses at the support, caused by earthquakes for a return period of 475 years.

Currently, the design of the tunnel's secondary lining is being carried out; nonetheless, preliminary analyses indicate that the lining's critical working conditions are located in the zones where the tunnel is deeper.

Seismic analysis. It is carried out for two working conditions: at a return period of 47.5 years for the primary lining's dynamic analysis (short term) and 475 years for the secondary lining (long term), using the method proposed by Wang and Parson (1993). Results indicate that deformation induced on the

concrete ring is very low, in the order of $\epsilon = 0.001$, for the longitudinal movement, and circumferential deformation of $\epsilon = 0.0003$ by oval shaping.

6.4 Special cases and studies

There are particular structures in the project that required a special design, such as in the assembly galleries. On occasions it was not possible to assemble the tunneling machine at surface, so assembly galleries had to be set up, with a horseshoe section 11.7 m high and 12.4 m wide, 25.5 m long. These galleries were built with a conventional tunneling system, meaning that at every step of the excavation, usually 1.5 m long, lining was installed. The support consisted of a layer of shotcrete 0.30 m thick, with steel arches set at 1 m intervals. Due to the tunnel geometry and soil's mechanical characteristics, tunnel excavation was done using a top heading and bench approach, and according to the soil's undrained shear resistance, fully grouted fiberglass dowels parallel to the tunnel axes were used to reinforce the excavation front.

These structures were analyzed with 3D numerical models of finite elements considering each constructive stage (Fig. 12).

On the other hand, special studies are being carried out on the behavior of dowels rings on the secondary lining using physical models (Fig. 13) (Aguilar *et al.*, 2010).

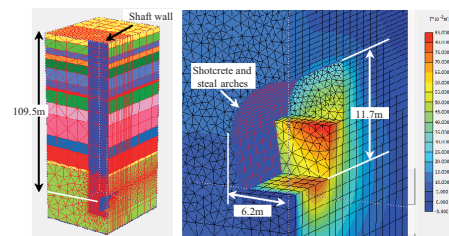


Figure 12. 3D numerical model of the analysis of the assembly gallery at L-17.

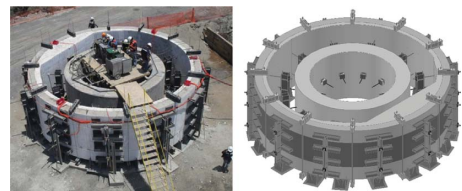


Figure 13. Study with instrumented physical models of the structural work of the voussoirs coupled to the secondary lining.

7 ANALYSIS AND DESIGN OF THE SHAFT EXCAVATION PROCESS AND LINING

In order to ensure the stability of the excavation and good construction and service conditions, attention must be paid to a number of ultimate and serviceability states (Auvinet *et al.*, 2010).

The failure mechanisms analyzed were: depth, lateral extrusion, sub-pressure, flotation, kicking, excavation advance without support.

Ultimate states include:

- Soil fracturing and slurry losses.* During the excavation of the annular trench, some incidents have been reported such as fluid losses or fracturing of the soil due to slurry pressure. In Mexico City soft clays, fracturing may appear when the slurry level is raised only one meter above the water table level. The construction of a concentric plastic concrete annular wall is helpful to prevent fracturing.
- Excavation stability.* The general stability of the excavation (progressive or total excavation, bottom general failure, kicking) can be assessed using standard analytical limit analysis methods such as those proposed by Nash & Jones (1963), Alberro & Auvinet (1984) and Tamez (2001). However, numerical methods are now generally preferred. Using for example the finite element method, it is possible to take into account the geometric and mechanical details of the problem with great accuracy. In this type of analysis, the selection of an adequate constitutive model is extremely important (Hejazi *et al.*, 2008). The most critical shear failure mechanism is generally a wall failure (Fig. 14a), although local extrusion of soft layers is also known to have happened in other excavations for the Mexico City subway system. On the other hand, when

a concrete wall is built around a previous the excavation, bottom shear failure is most critical (Fig. 14b). When analyzing this mechanism, the fact that the bottom of the excavation's expansion induces a progressive increase of the water content and a reduction of the soil's shear strength should be taken into account.

- Bottom uplift failure.* In most cases, the bottom of the excavation is located slightly above the first hard layer. In this relatively pervious layer (typical permeability coefficient $k = 10^{-6}$ m/s), pore pressure is generally partially abated due to pumping of potable water for the city. Failure of the excavation bottom due to the uplift pressure is however a clear possibility. The safety factor can be obtained comparing the uplift pressure with the weight of the soil in the excavation bottom and of the slurry if it was used. It should however be taken into account that the weight of the slurry induces a pore pressure increment in the pervious layer. The transient conditions prevailing when the slurry level suddenly goes down can lead to the development of unfavorable seepage forces towards the excavation. This situation can be easily simulated performing transient flow analyses using the finite element method (Fig. 15a).

When the excavation rests directly on the hard layer, the granular material of this layer can present a boiling condition when the vertical gradient due to lowering of the slurry level reaches a critical value.

To cancel any possibility of uplift failure and buoyancy condition, electrosmotic water pumping from the hard layer has been used by one of the contractors to control hard layer pore pressure. Finite element modeling and instrumentation with piezometers have been used to assess the efficiency of this solution (Fig. 15b).

- Floating of finished structure.* When the construction of the shaft is finished the structure may float in certain conditions. This happens when the Archimedes thrust is larger than the sum of the weight of the structure and the lateral friction between soil and concrete developed on the shaft's surface perimeter. This is more likely to

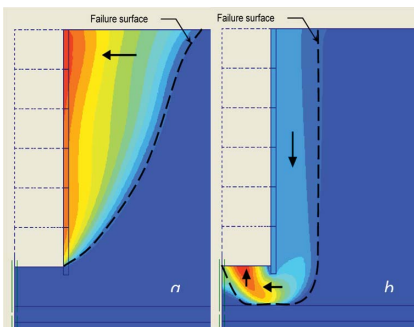


Figure 14. Potential shear failure mechanisms (Contour displacements): (a) without concrete wall (b) with concrete wall.

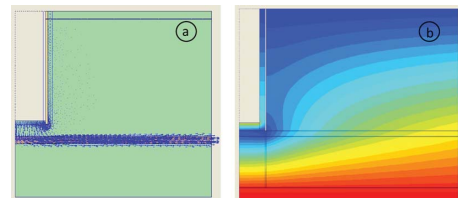


Figure 15. FEM simulations of: (a) Transient flow conditions in pervious layer and (b) Pumping in the hard layer to control uplift thrust (hydraulic head contours).

happen with shafts of large diameter, since lateral friction is proportional to shaft diameter, whereas the Archimedes thrust grows as the diameter squared. When necessary, the structure must be ballasted and/or the shaft wall's thickness increased to avoid flotation.

- e. *Behavior of shafts against negative friction.* If the pore pressure decreases in superficial clay deposits located down to 40 m depth, it will generate negative friction on the shaft skin. The negative friction could be calculated using the following equation (Zeevaert, 1983):

$$NF = \pi D \cdot K_\phi \cdot \int \sigma_0 \cdot dz_i$$

where, NF is the negative friction on the shaft skin, D is exterior diameter, K_ϕ is the long term lateral earth pressure for each stratum, $K_\phi \approx 0.3$, and $\int \sigma_0 dz_i$ is the area of the diagram of vertical effective stresses according to the total abatement. It is also possible to evaluate the effect of this lateral force using FE Method. Serviceability limit states are also important:

- f. *Movements induced in neighboring buildings during construction.* In an urban environment, neighbors are frequently worried that soil displacements induced during shaft construction could damage their property. Careful attention must be given to this problem. However, displacements computed using finite element modeling are small and, in normal conditions, excavation by the flotation method should not affect other constructions. This has been confirmed by instrumentation measurements on many sites.
- g. *Long term behavior.* A much more critical aspect is the apparent protruding of the shaft with respect to the surrounding ground that may occur due to the contribution of the upper clay formation to the regional subsidence. A protruding rate of 18 cm per year may be expected in shafts L-0 and L-1. This is a very compelling reason to keep the shaft away from important constructions whenever possible.
- h. *Seismic behavior.* The seismic behavior of the shafts considering an event with return period of 475 years was also studied using an analytical approach proposed by Pérez & Avilés (2010). Results show that seismic loads are the most critical condition, mainly in deep shafts, but using 3D numerical modeling the working conditions of the support are substantially lower (Fig. 16, Rangel *et al.*, 2010).

A very important point during an earthquake is the behavior of the tunnel-shaft joint because these structures are moving in a different way. Due to

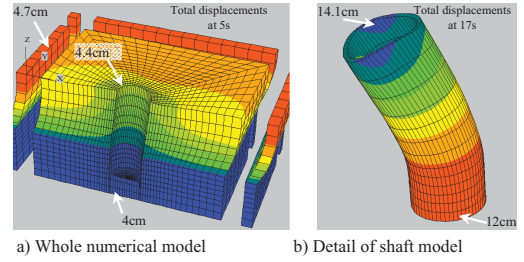


Figure 16. Three dimensional numerical difference finite model using flac3D. Total displacement diagrams determined at 5 s (a) and 17 s (b) of the earthquake signal.

high stress concentration during seismic loads this project does not consider the joint between tunnel and shaft.

8 MONITORING AND BEHAVIOR

The TEO instrumentation program includes the following measurements:

- a. *Convergences.* Using extensometers, the shortening and lengthening of each of the tunnel's primary lining rings are measured on the vertical and horizontal axes.
- b. *Surface leveling.* Measurement of settlements on lines transverse to the tunnel's outline, and edifications.
- c. *Instrumented dowels rings.* Along the already built tunnel five dowel rings have been instrumented by means of: seven joint measurers, four pressure cells, eight deformation meters for steel, and eight deformation meters for concrete.
- d. *Measurement of pore pressure in the soil.*
- e. *Measurement of subsoil movements with inclination meters.*
- f. *Measurement of the tunneling process variables:* front pressure, advance speed, alignment, volume and pressure of injection mortar, etc.

Currently, the primary support has been excavated and placed in almost all the shafts, whereas the tunnel is excavated with the primary lining only on its first 243 m from shaft L-0.

8.1 Tunnel

The zone where the tunnel has already been excavated is characterized by consisting totally of very compressible clays, with low shear resistance and maximum humidity contents of 400% and regional subsidence of 18 cm/year. Also, this zone is the most critical from the point of view of affectation to the existing infrastructure and the edifications at the surface (mainly homes). In effect, the tunnel's

keystone is located between 15 m and 25 m depth, and a vehicle bridge with piles is crossed passing only 2.5 m away from the piles of one of the supports.

Therefore, this section has been extensively instrumented: there are instrumented dowel rings approximately every 30 cm, leveling lines have been installed at surface and buildings, and the convergences on each ring are measured with more frequency.

Fig 17 shows a summary of the convergence, injection pressure and volume measurements carried out during 8 months. It shows that the tendency of the measurements of vertical and horizontal convergences is to stabilize between the values of 4 cm and 5.5 cm, save at some special points that report values of up to 7 cm. It is important to comment that no cracks or fissures haven observed on the body of any ring, or aperture of the joints, transverse of longitudinal, nor any filtrations that lead to a condition of loss of sealing.

It has also been observed that there are abrupt convergence increases that are correlated with these events:

- Extraordinary event, tunnel flooding: between 4 and 5 February 2010
- Start of rain season: June 2010

- Earthquake 6.4°: 30 June 2010
- Excavation resumed: 4 August 2010

These events caused convergence increases in small time lapses. For example: in the case of ring No. 37, Figure 18, the first period, that corresponds December-January, the record shows a deformation speed $\Delta\delta h = 16$ mm/month, presenting a jump at the end of the period that coincides with the tunnel's flooding. Then, the deformation speed tends toward 4 mm/month between February and May, and drops to 2.3 mm/month from May onward, with a tendency to stabilization. The events marking the start of the rain season and the earthquake have been reflected with small convergence increases.

The cases where high convergence values (between 4.5 cm and 7 cm) occur are associated with deficiencies in the constructive process, such as injection pressure or volume decrease of the project at this section, 1.5 bar and 7.55 cm³ respectively. In particular cases, such as the tunnel's nearness to the bridge's foundation piles, injection volume increases have been measured of up to 12.5 m³.

Average convergences measured to date at this section, 4 cm to 5.5 cm, are slightly higher than the design measurements of 3 cm to 4.2 cm.

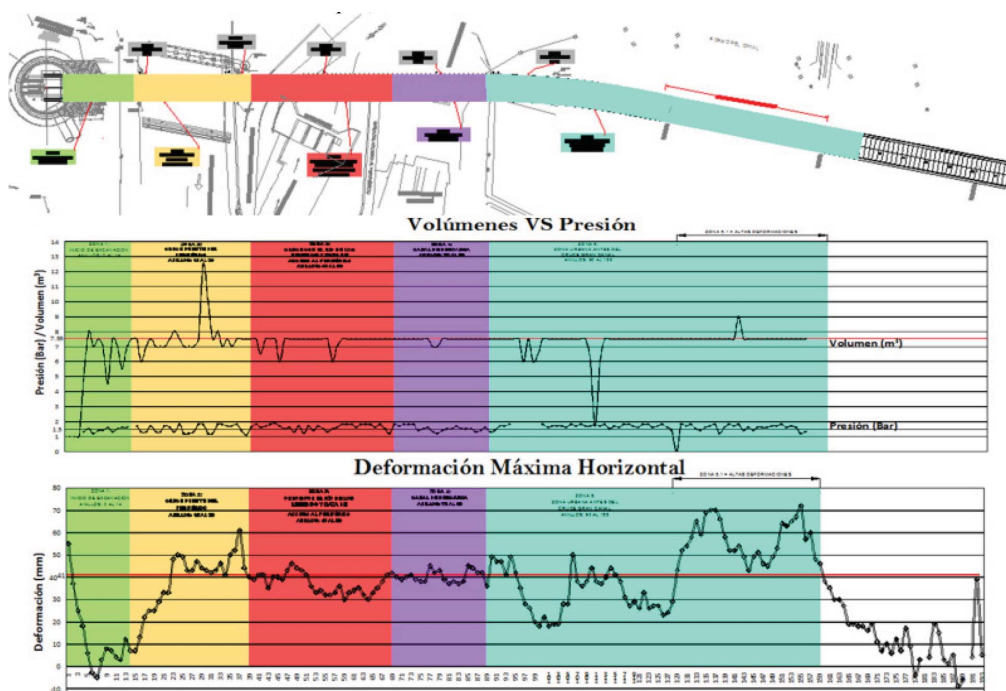


Figure 17. Measurements made at the tunnel after 8 months of construction: (a) plan location, (b) injection pressures and volume, (c) horizontal convergence and (d) vertical convergence.

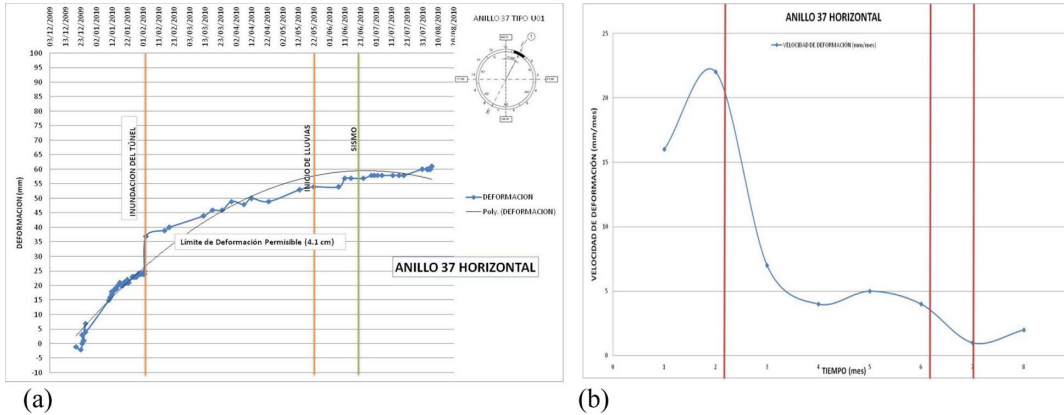


Figure 18. Convergence measured at voussoir ring 37: (a) time vs horizontal convergence diagram, (b) time vs deformation speed diagram.

With respect to surface land settlements, two zones have been observed: the first, at between 0 and 50 m of tunnel, settlements are in the order of 13 cm, with a maximum of 14.3 cm, whereas for the second, between 50 m and 243 m, reported settlements were of the order of 4.4 cm, with a maximum of 6.4 cm. Settlements measured at the first zone are important, and are a product of the vehicle bridge-tunnel's interaction.

8.2 Shafts

Shaft behavior in general has been satisfactory from the point of view of stability during construction and useful life; nonetheless, there have been constructive problems, mainly with the tolerance of deviation of each diaphragm wall panel and entrapment of the trench excavating machine.

The cases where these problems occurred were at shaft L-5, after crossing a very hard stratum, and then when finding a soft and deformable stratum, and at the deepest shafts, as in L-20, of 155 m depth, where a diaphragm wall was built for the first 120 m and then using the conventional method and immediate placing of the support.

9 CONCLUSIONS AND RECOMMENDATIONS

Exploration: Exploration techniques for samples and lab tests used in conventional Mexican engineering produced adequate results at depths of less than 60 m. For more depth, new technologies were required, such as measuring shear wave velocity

by means of the SPAC geophysical technique, the use of a presiometer, phicometer, triple barrel samplers, etc.

Design: The design strategy has been congruous with what has been observed during the development of the construction work, with convergences similar to what was indicated at the design stage, and observing the integrity of the dowel rings.

In the section of clayey soils and coverage between 28 m and 40 m, it was observed that the value of flexion rigidity EI used to consider the joints between dowels and dowel rings varies between 10% and 15%.

Instrumentation: It was observed that pore pressure dissipation with the passing of the tunneling machine in clayey soils was quick, taking a day at most. The calculations have been consistent with what the observed during the construction.

Constructive processes: For the tunnels excavated in clayey soils, surface settlements are fully related to the tunnel's constructive process. In effect, the adequate selection of pressure, volume and type of dosage of the injection mixture for the annular space between dowel and soil avoids generating important settlements, as otherwise these settlements can affect neighboring buildings. Other aspects to care for are the pressure applied at the excavation front, and an homogenous injection process along the entire space. For the case of the TEO, minimal pressure to apply at the front was determined following these criteria:

- $p_f = u + 0.5 \text{ kg/cm}^2$
- $p_f = \sigma_v \times k_a + u + 20 \text{ kPa}$.

Also, it was considered that $p_{iny} = p_f$.

Geotechnical issues: The main geotechnical problems during the design and construction in soft soils were:

- The dynamic amplification and subsidence problems in Mexico City clays
- Tunneling in an urban area with very soft soils
- Tunneling soils at 50 m and 155 m deep
- Having mixed soil condition like sandy silt and basalts lens or clay lens in sandy silt hard layers
- The construction of deep shafts (up to 160 m) in difficult soil condition

For tunneling in soft soils, the surface settlements are fully associated with the tunnel construction process. In fact, the proper selection of pressure, volume and the grout for the annular injection between soil and lining prevent the generation of unacceptable settlements. Other aspects to take into account are the pressure applied on the excavation face and be careful to have a uniform injection around the tunnel.

ACKNOWLEDGEMENTS

We would like to thank to the organizing committee for the invitation to this symposium, especially to Professor Richard Kastner and Professor Stefano Aversa. A recognition as well to the working team who dedicate most of their time to the construction of this important project.

This article is a contribution of technical committee TC-214.

REFERENCES

- Aguilar, O., L. Mendoza, E.A. Tavera, Y. Alberto and J. Morelos (2010), Load test on a real scale model of a tunnel with secondary lining, *National Soil Mechanics Meeting*.
- Alberro, J. and G. Auvinet (1984), Construcción de estaciones de Metro a gran profundidad en las arcillas del Valle de México (Construction of deep subway stations in Mexico City valley clays), *Technical Report to COVITUR*, December, Mexico.
- Arias, F. (1997), Confiabilidad de trincheras estabilizadas con lodo (Reliability of slurry trenches), *Master degree thesis*, División de Estudios de Posgrado de la Facultad de Ingeniería, UNAM, Mexico.
- Auvinet, G. and J.F. Rodríguez (2004), Análisis de lumbreras cilíndricas sometidas a cargas locales (Analysis of shafts subjected to local loads), *Proceedings, XXII National Soil Mechanics Meeting*, Sociedad Mexicana de Mecánica de Suelos, Vol 2, Guadalajara, Mexico, pp 317–322.
- Auvinet-Guichard G., J.F. Rodríguez-Rebolledo and J.L. Rangel-Núñez (2010), Construction of deep tunnel shafts in Mexico City soft clays by the flotation method, *Acta Geotechnica*, 5, Springer-Verlag, DOI 10.1007/s11440-010-0115-2, pp 63–68.
- Auvinet Guichard, G. (2010), Doscientos años en la historia de la ingeniería en México (Two hundred years in the history of engineering in Mexico), *Separata*, Fundación ICA, Mexico, DF.
- Comulada-Simpson, M., and U. Maidl (2010), Design and structural analysis of lining segments in soft soils. *International symposium on Tunnels and Shafts*, Mexican Society of Soils Mechanics and Mexican Association of Underground Works and Tunnel Engineering, Mexico, DF.
- Farjeat Paramo, E. (1975), Memoria Técnica de las Obras del Drenaje Profundo del Distrito Federal, *TUNEL S.A. de C.V.*, Mexico DF.
- Google-Earth (2011), Electronic maps.
- Hejazi Y., Dias D. and Kastner R. (2008) Impact of constitutive models on the numerical analysis of underground constructions, *Acta Geotechnica*, 3, 251–258 DOI 10.1007/s11440-008-0056-1.
- Jaky, J. (1944), The coefficient of earth pressure at rest, *J. Soc. Hungarian Architects Eng.*, 7–355–358.
- Jaw-Nan Wang and Parsons Brinckerhoff Inc. (1993), *Seismic design of tunnels: a simple state-of-the-art design approach*, Parsons Brinckerhoff Inc., One Penn Plaza, New York.
- Juárez, M., G. Auvinet, F. Hernández and E. Méndez (2010), Contribución a la caracterización geotécnica de la zona norte de la cuenca de México (Contribution to geotechnical characterization of the north part of Mexico Basin), *Memorias Técnicas, XXV Reunión Nacional de Mecánica de Suelos e Ingeniería Geotécnica*, Sociedad Mexicana de Ingeniería Geotécnica, Acapulco, Gro., Mexico.
- Mooser, F., A. Montiel and A. Zúñiga (1996), Nuevo mapa geológico de las cuencas de México, Toluca y Puebla (New geological map for Mexico, Toluca and Puebla basins), *Comisión Federal de Electricidad*, ISBN: 968-7780-00-2, Mexico DF.
- Mooser, F. (2010) Modelo Geológico del Túnel Emisor Oriente (Geological model of TEO), COMISSA, Mexico, DF.
- Nash J.K.T.L. and G.K. Jones (1963), The support of trenches using fluid mud, grouts and drilling muds in *Engineering Practice*, Butterworths, London, pp 177–180.
- Perez-Rocha, L.E. and J. Avilés López (2010), Determination of seismic actions in shafts buried in soft soils, *International Symposium of Tunnels and Shafts* in Mexico City, SMIG and AMITOS, Mexico.
- Rangel, J.L., U. Iturrarán V, A.G. Ayala and F. Cervantes (2005), Tunnel Stability analysis during construction using a neuro-fuzzy system, *Int. Jour. Num. An. Meth. in Geomech.*, 29: 1434–1456.
- Rangel-Núñez, J.L., G. Auvinet-Guichard and E. Tamez-González (2007), A simple criterion to evaluate tunnel stability during construction, *ECCOMAS Thematic Conference on Computational Methods in Tunneling*, J. Eberhardsteiner et al (eds.), Vienna, Austria.
- Rangel-Núñez, J.L., S. Martínez Galvan, N. Salmiento-Solano and E. Ovando-Shelley (2010), “Dynamic analysis of shafts in Mexico City deposits,” *International Symposium of Tunnels and Shafts* in Mexico City, SMIG and AMITOS, Mexico.

- Tamez, E., J.L. Rangel Núñez and E. Holguín (1997), *Diseño Geotécnico de Túneles (Geotechnical design of tunnels)*, TGC Geotecnia, Mexico DF. ISBN 9685571007.
- Tamez, E. (2001) *Ingeniería de Cementaciones. Conceptos Básicos de la Práctica* (Foundation Engineering. Basic Practice Principles), TGC Geotecnia, Mexico.
- Wilson, E. (1965), *Structural Analysis of Axisymmetric Solids*, American Institute of Aeronautics and Astronautics Journal, Vol. 3–12 December, USA, pp 2269–2273.
- Zeevaert, L. (1983), *Foundation Engineering for Difficult Subsoil Conditions*, 2nd ed., Van Nostrand Reinhold.